Microstructure of ECAE-Processed Copper after Long-Term Room-Temperature Storage

O.V. MISHIN and A. GODFREY

The microstructure in two copper samples processed by equal channel angular extrusion (ECAE) using either 90 deg rotations between passes (route Bc) or without rotations (route A) has been examined following storage at room temperature for a period of 8 years. In both samples the deformation microstructure was significantly heterogeneous, as indicated by large differences between the extent of microstructural refinement from place to place along the center line of the extrusion. The route Bc sample, however, showed a greater degree of heterogeneity, though with an overall lower degree of refinement. A number of recrystallized grains were seen in both samples, with a greater recrystallized fraction observed for the route Bc sample. The effect of the processing route on the microstructure and consequences of the observed heterogeneity for microstructural characterization of ECAE-processed material are discussed.

I. INTRODUCTION

THE strong demand for materials with advanced properties has in recent years stimulated the development both of new materials and of new processing techniques. In response to this demand several novel deformation techniques have emerged, which have resulted in a large number of publications reporting unusual physical and mechanical properties. Equal channel angular extrusion (ECAE)[1,2] is one such technique and has attracted significant attention. A large amount of research work on the microstructure resulting from ECAE processing has been accumulated and these materials are now being considered for commercial applications. Successful commercialization of ECAE-processed materials will, however, require not only the development of a suitable microstructure in the as-processed condition, but also the ability to maintain this microstructure over significant periods of time. It is known that microstructures of heavily deformed metals are sometimes unstable even at room temperature. For example, heavily-drawn thin wires of pure copper used in electrical and electronic products can recrystallize during aging at room temperature,[3,4] which leads to a deterioration in their mechanical properties. To stabilize the deformation structure, changes in the chemical composition or in the thermomechanical history are usually required. Data in the literature regarding the microstructural stability of ECAE-deformed copper are very inconsistent. While commercially pure copper after multipass ECAE is often considered stable at temperatures below 100 °C,[5,6] there have been several communications[7–10] describing large grains and room-temperature partial recrystallization after ECAE processing.

To evaluate the long-term room-temperature stability of ECAE-processed copper, samples kept at room temperature for a period of 8 years have been re-investigated following a transmission electron microscope (TEM) analysis of their microstructures in the as-deformed condition. A sample extruded with 90 deg rotations between passes (route Bc) was originally used for a TEM investigation of boundary misorientations in the as-processed condition.[11,12] The as-deformed microstructure of this sample did not contain coarse recrystallized grains, but it was very heterogeneous; both the local morphology and the fraction of high angle boundaries (HABs) varied significantly in different regions of the sample. A TEM investigation was also carried out on a sample prepared using route A, although its microstructure was not analyzed in our previous publications. To extend knowledge of the length scale of the sample heterogeneity and to identify recrystallized grains, orientation mapping of large areas is performed in this work using the electron backscatter diffraction (EBSD) technique.

O.V. MISHIN, Senior Scientist, is with the Center for Fundamental Research: Metal Structures in Four Dimensions, Materials Research Department, Risø National Laboratory for Sustainable Energy, Technical University of Denmark, DK-4000 Roskilde, Denmark. Contact e-mail: olmishin@lycos.com A. GODFREY, Professor, is with the Laboratory of Advanced Materials, Department of Materials Science and Engineering, Tsinghua University, Beijing 100084, P.R. China.
Manuscript submitted March 26, 2008.
Article published online October 1, 2008.

II. EXPERIMENTAL

Two 99.96 pct pure copper samples, each deformed by eight ECAE passes through a die with channels intersecting at 90 deg and a rounded outer corner ($R = 45$ deg) were used for this study. One of the samples was processed without rotations (route A - sample A); the other sample was processed with sequential 90 deg rotations between each ECAE pass (route Bc - sample B). The specimens

were stored at room temperature for 8 years in the form of mechanically polished sections and TEM foils.

The longitudinal side section, *i.e.*, the section that contains the extrusion direction and normal direction (ED-ND) of the billet, was prepared for EBSD analysis in this investigation. In order to remove the surface layer, the specimens were polished mechanically and then electrochemically. The EBSD measurements were performed using a Zeiss Supra-35 field-emission gun scanning electron microscope (FEGSEM) equipped with the Channel 5 EBSD system (Oxford Instruments-HKL Technology, Hobro, Denmark). At first, a step size of between 60 to 70 nm was selected for orientation mapping covering a total area of ~11,000 μm^2 in each sample. This area is comparable to the area originally inspected in the TEM, where 3 foils were examined for each sample. To estimate a typical transparent foil area, 2 foils used in the original TEM experiment[11,12] were re-examined in a JEOL*-

---

*JEOL is a trademark of Japan Electron Optics Ltd., Tokyo, Japan.

2000FX TEM operating at 200 kV, which gave an average foil area suitable for detailed analysis of 8000 μm^2. Thus, the total area inspected in the original TEM study for each sample is estimated to be 24,000 μm^2. As sample B was found to be much more heterogeneous than sample A, two additional maps from sample B were collected using larger step sizes of 0.4 and 0.5 μm. These coarse-step maps covered ~150,000 μm^2 and were only considered for establishing the scale of the microstructural heterogeneity, but were not used for quantitative analysis of the boundary misorientations. All maps were collected from near the center line of the extrusions.

The heterogeneity in the deformed microstructure was analyzed in the following manner. First, the subset of each map containing recrystallized material was identified. This was achieved by first carrying out a grain reconstruction process using a boundary definition of 10 deg. Recrystallized regions were then identified automatically as those reconstructed grains with an average internal misorientation of less than 1.5 deg and with an area greater than 0.5 μm^2. A small number of grains that could clearly be identified as recrystallized (from the presence of twin boundaries) were missed using this procedure and these were added manually to the recrystallized area subset. The remaining deformed material was then divided into two subsets that were subsequently used for identifying regions containing predominantly high-angle misorientations (high-misorientation regions (HMRs)) and regions containing predominantly low-angle misorientations (low-misorientation regions (LMRs)). This was achieved by first repeating the reconstruction process, this time using a boundary definition of 5 deg. The detected subgrains in the deformed material were then divided into two subsets corresponding to those reconstructed subgrains with areas greater than 2.5 μm^2 (the LMR subset) or smaller than 2.5 μm^2 (the HMR subset). For quantification of the

extent of recrystallization, the area fraction of recrystallized grains in each sample was also determined from backscattered electron (BSE) images using an image-analysis software package.

III. RESULTS

A small number of recrystallized grains were found in both of the deformed samples examined. In subsequent sections, the microstructure in the deformed regions is described, followed by a description of the extent and nature of the recrystallization in the samples.

A. *Characterization of Deformation Structures*

An example EBSD data set for one of the investigated regions in sample A is shown in Figure 1. It is seen that the microstructure is in general composed of elongated structures inclined close to the ED. The directionality in the microstructure is disrupted in some places by shear bands lying at an angle of 45 to 50 deg to ED. From the BSE images, the boundary spacing along the ND was found to be ~0.2 μm. The texture of sample A (Figure 3(a)) was a typical shear texture, similar to those reported elsewhere for samples deformed by ECAE
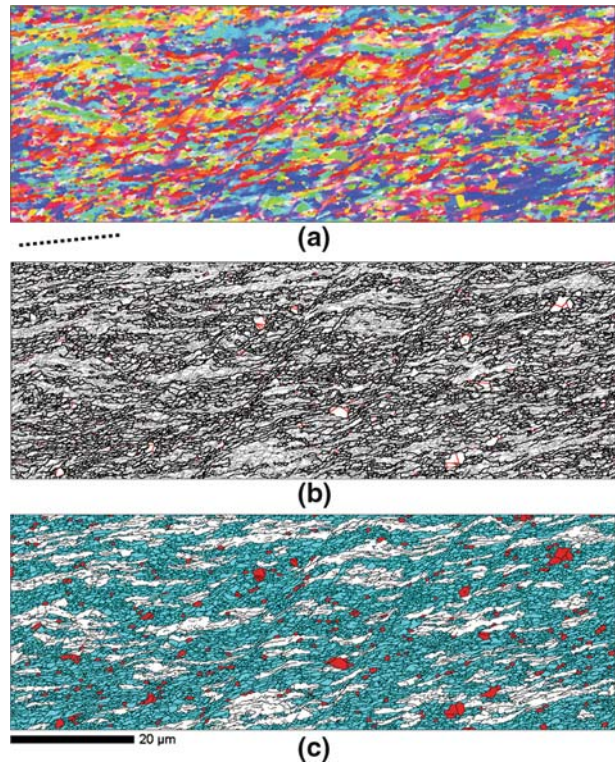

Fig. 1—EBSD data for a region in the sample extruded using route A: (*a*) orientation map (colors correspond to the crystal direction parallel to ND); (*b*) misorientation map showing twin boundaries in red, HABs (>15 deg) in black, and 2 to 15 deg misorientations as thin gray lines; and (*c*) map showing the microstructure divided into high-misorientation (blue), low-misorientation (white), and recrystallized (red) regions, with misorientations of >5 deg shown in black. Extrusion direction is indicated by dashed line.

Table I. Microstructural Parameters Obtained from EBSD Analysis of Samples A and B

Sample	Average HAB Spacing (nm) ND/ED	HAB Fraction** (Pct)	Area Fraction (Pct)			Mean Misorientation** (Deg)	
			HMR*	LMR*	Recr*	HMR*	LMR*
A	540/940	46	60	38	2	22	6
B	780/1200	37	40	55	5	20	5

* HMR (high misorientation region), LMR (low misorientation region), and Recr (recrystalized region) defined according to the procedure given in Section II.

** The mean misorientation and high angle boundary (HAB) fraction are both calculated using a minimum misorientation (lower threshold) of 2 deg.

using route A.[13] The average HAB spacings along the ND and ED were determined from the fine step-size EBSD maps as ~0.5 and 0.9 μm respectively, with a corresponding average value of the HAB fraction of 46 pct (Table I). The fraction of HABs is defined here as $L_A > 15$ deg$/L_A > 2$ deg, where $L_A > \theta^*$ represents the length per area of boundaries with misorientation greater than θ^*. As can be seen in Figure 1(b), the HABs are not uniformly distributed. Instead, the microstructure consists of regions containing many HABs and regions containing a low density of HABs.

These regions where the microstructure is either less refined or more refined are shown more clearly in Figure 1(c), constructed following the procedure described in Section II. Blue areas in the figure correspond to HMRs and white areas correspond to LMRs. Areas in red in Figure 1(c) indicate recrystallized grains. The corresponding area fractions are listed in Table I, together with the average boundary misorientation inside the low-misorientation and high-misorientation regions.

An example fine step-size EBSD data set for one of the regions characterized in sample B is given in Figure 2. In this region the high-angle misorientations are mainly associated with two sets of boundaries. One set is produced by boundaries at 50 to 55 deg to the ED. The inclination of the second set is at 20 to 25 deg to the ED. It appears that this map represents orientations of a single grain divided into cell blocks by intersecting sets of boundaries. The orientation differences between the cell blocks were measured relative to the point marked "1" in Figure 2(a) (*i.e.*, 1-2,1-3,...,1-9) and were found to be small: 12, 3, 9, 12, 8, 5, and 7 deg. Furthermore, Figure 3(b) confirms that crystallographic texture in this region is dominated by one orientation.

Figures 2(b) and (c) demonstrate the heterogeneity in this data set. It is clear that the degree of heterogeneity is significantly different from that seen in Figure 1 (sample A). The fraction of HMRs is considerably smaller than that in sample A, while the fraction of recrystallized grains is larger. Somewhat different characteristics were seen in other parts of this sample. Another region from sample B is shown in Figure 4. In this region the LMRs and HMRs are mixed more uniformly, and the fraction of recrystallized grains is much smaller. For sample B the average HAB spacings along the ND and ED were determined as ~0.8 and 1.2 μm, respectively, with a corresponding average value of the HAB fraction of
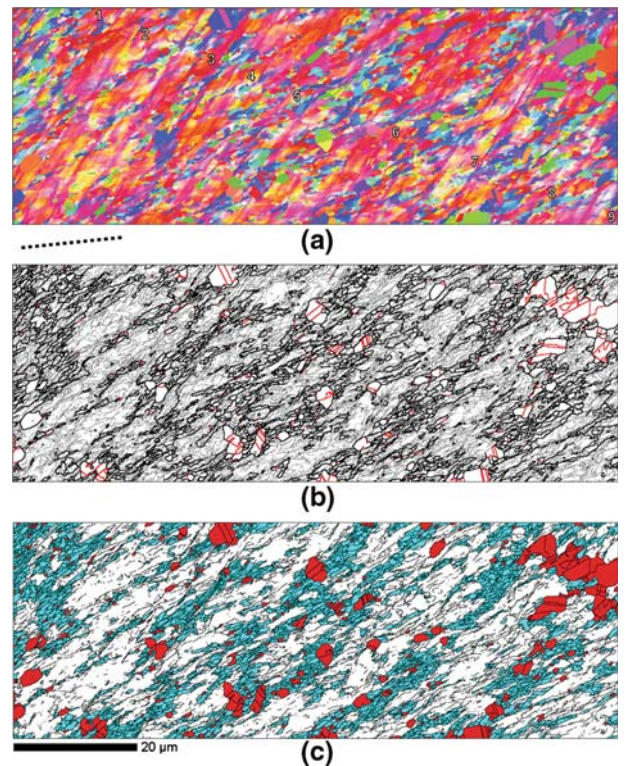

Fig. 2—EBSD data for a region with a large number of recrystallized grains in the sample extruded using route Bc. (*a*) Orientation map (colors as for Fig. 1). Digits indicate points along a linear traverse, where orientation differences were measured (refer to text). (*b*) Misorientation map, showing twin boundaries in red and other HABs in black. Thin gray lines correspond to 2 to 15 deg misorientations. (*c*) Map showing the microstructure divided into high-misorientation (blue), low-misorientation (white), and recrystallized (red) regions, with misorientations of >5 deg shown in black. Extrusion direction is indicated by dashed line.

37 pct (Table I). The fraction of LMRs, HMRs, and recrystallized regions in sample B are also given in Table I, where it is seen that these fractions are significantly different from those for sample A.

To give a clearer impression of the scale of microstructural heterogeneities in sample B, a map from a large area of 0.5×0.25 mm^2 collected using a coarse step size of 0.5 μm is presented in Figure 5. Such a step size does not allow individual subgrains to be identified, however the map illustrates well the considerable local variations in the boundary alignment as well the extent
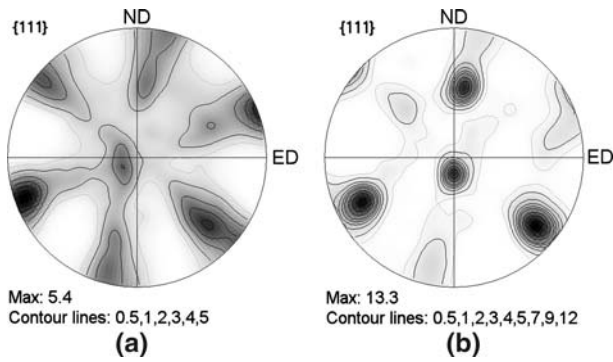
Fig. 3—{111} pole figures for the regions presented in Figs. 1 and 2: (*a*) sample A (Fig. 1) and (*b*) sample B (Fig. 2).

Fig. 5—Orientation map produced using a step size of 0.5 μm showing the scale of heterogeneity over an area of 0.5×0.25 mm^2 in sample B. The scale bar is 200 μm.
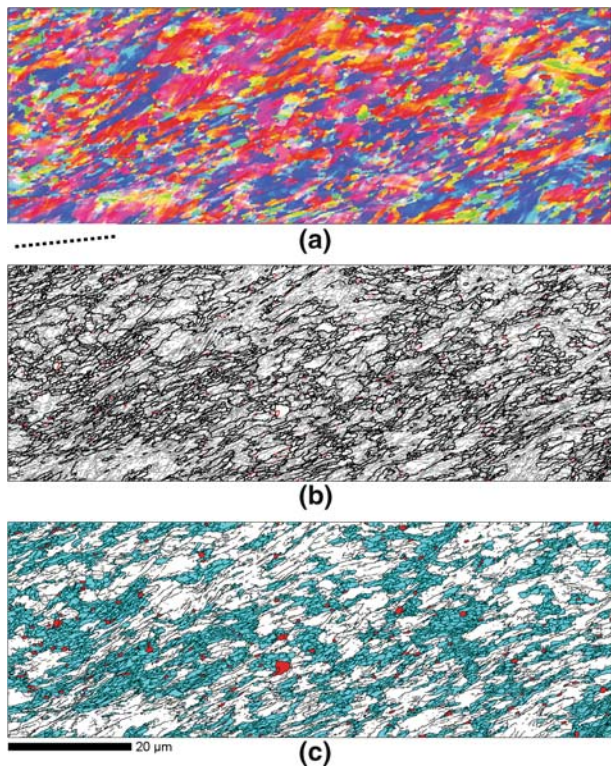

Fig. 4—EBSD data for a region with a small number of recrystallized grains in the sample extruded using route Bc. (*a*) Orientation map (colors as for Fig. 1). (*b*) Misorientation map, showing twin boundaries in red and other HABs in black. Thin gray lines correspond to 2 to 15 deg misorientations. (*c*) Map showing the microstructure divided into high-misorientation (blue), low-misorientation (white), and recrystallized (red) regions, with misorientations of >5 deg shown in black. Extrusion direction is indicated by dashed line.

of volumes with similar orientations. A number of large areas (in some cases more than 3000 μm^2) each with a similar orientation were found in the map.

B. *Characterization of Recrystallized Grains*

Evidence of recrystallization was observed in both of the ECAE samples examined in this study. In the EBSD data recrystallized grains could be detected based on
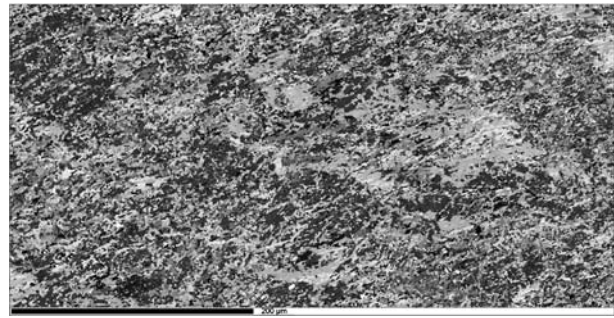
several features. These include the size of the recrystallized grains (being larger than the size of cells and subgrains in the deformed matrix), the higher EBSD pattern quality inside recrystallized grains, and the fact that the recrystallized grains are not subdivided by low-angle boundaries (hence giving a low value for the internal misorientation). Additionally, in many places recrystallized grains can be identified by the presence of twin boundaries (shown in red in the misorientation maps of Figures 1, 2, and 4.). Note that, based on results of a previous characterization of annealing twins in copper,[14] only boundaries with deviations <3 deg from the ideal twin misorientation are classified in this work as twin boundaries. This approach is more restrictive than the commonly used Brandon criterion that allows a very generous maximum deviation for the $\Sigma 3$ boundary, 8.66 deg.

In both samples, recrystallized grains were typically observed within HMRs, either at shear bands, at extended boundaries, or at their intersections (Figure 6). To allow a better sampling of the wide variation in the amount of recrystallized grains found in different regions of sample B, the extent of recrystallization was also quantified from BSE images. It should be noted that only recrystallized grains larger than ~1 μm could be recognized unambiguously in the BSE images used for the evaluation. The analysis gave average values of 2 and 7 pct for samples A and B, respectively. These values are similar to those obtained from the EBSD data (Table I). Thus, both BSE images and EBSD data provide clear evidence that large recrystallized grains are more frequent in the sample deformed using route Bc. It was also apparent that local variations in the fraction recrystallized were greater in sample B. In the individual BSE images recorded from sample B the area fraction of recrystallized grains varied from 0.8 to 30.6 pct, while in sample A the variation was less significant, 0.6 to 3.7 pct (Figure 7).

IV. DISCUSSION

Three findings in this study are considered to be important: (1) significant heterogeneity is seen in the deformed microstructure in both ECAE-processed
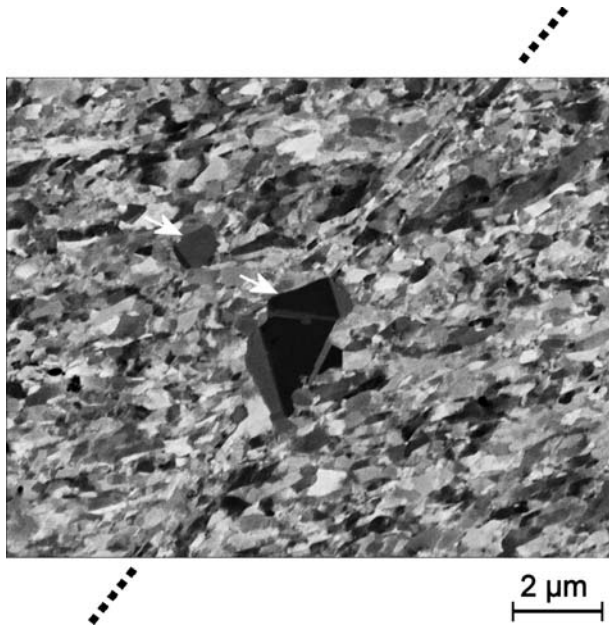
Fig. 6—BSE image showing recrystallized grains (indicated by arrows) at local heterogeneities in sample A. Dashed line indicates a shear band in which a larger recrystallized grain is observed. Note narrow annealing twins in both grains.
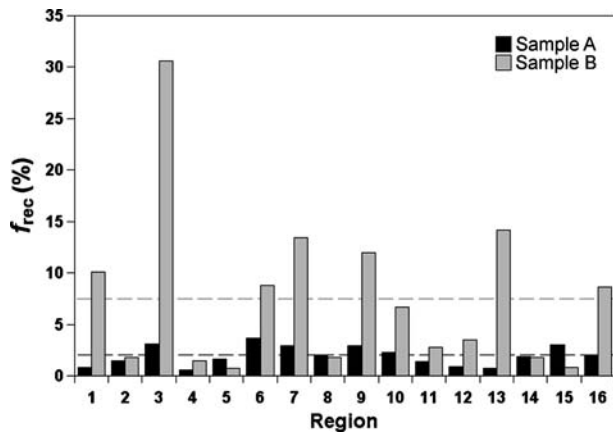

Fig. 7—Variation in the area fraction of recrystallized grains for samples A and B as measured from BSE images and EBSD maps. Each region is 3100 to 3400 μm^2 large. Dashed lines correspond to the average values from all regions examined.

samples; (2) the sample extruded with 90 deg rotations around the longitudinal direction is more inhomogeneous and contains fewer HABs than the sample deformed without rotations; and (3) both samples were found to be partially recrystallized after long-term storage at room temperature. These findings and implications for microstructural characterization of ECAE-deformed materials are discussed in the following subsections.

A. Microstructure in Copper after Different ECAE Routes

The influence of the processing route on the microstructural evolution during ECAE has been debated for

several years. For routes A and Bc used in this experiment, there are two opposing views on their effectiveness in terms of grain refinement. In many reports (reviewed in Reference 15) route Bc is claimed to most rapidly create an array of equiaxed grains separated by high-angle grain boundaries. It is important to note that much of the early work that led to this conclusion was performed using selected area diffraction (SAD) patterns in which only limited information is available about the actual boundary misorientations.[16] In contrast, more detailed studies of Al-alloys carried out later using EBSD by Gholinia et al.[17] and Berta et al.[18] showed that processing with 90 deg rotations was less efficient in forming new HABs than ECAE without rotations. In those publications, the reduced rate of HAB formation after deformation with rotations between passes was explained in terms of redundant strain.[17,18] It should be mentioned that Gholinia et al. and Berta et al. used a 120-deg ECAE die in their experiments. It has subsequently been suggested[19] that conclusions regarding the efficiency of different ECAE routes obtained on samples deformed using such a die cannot be extended to samples processed through 90 deg dies.

It is clear therefore from an examination of the published literature that the dependence of the processing route on the efficiency of refinement is still not fully understood. The data of the current investigation on copper show that for a 90 deg die route A after eight ECAE passes generates a higher frequency of HABs and a smaller average HAB spacing than route Bc, and imply that the heterogeneity in the microstructure must be considered when making such comparisons. Our results are in agreement with the simulation data of Beyerlein et al.,[13] who predicted that route Bc (for which the original element shape is restored every fourth pass) should give less refinement than route A. It is noteworthy that the original grains can still be distinguished in some locations of the route Bc sample even after a strain of ~8 (Figure 2).

The analysis of the EBSD data shows a significant degree of heterogeneity in the deformation microstructure of both samples, as reflected by large variations in the degree of microstructural refinement. This heterogeneity has been quantified in the present study by identifying high-misorientation and low-misorientation regions, according to the procedure described in Section II. The average misorientation angle within the HMRs is in the range 20 to 22 deg, whereas in the LMRs the average misorientation angle is only 5 to 6 deg. This testifies that the orientation spread is much weaker in the LMRs than in the HMRs. Thus, it is clear that even at high ECAE strains there are large areas of the microstructure that are refined to an extent more typical of samples deformed to low strains. Although this heterogeneity is seen in both samples, the route A sample contains a significantly higher fraction of the HMRs (60 pct compared to 40 pct for the route Bc sample), and this difference accounts for the overall increased refinement for sample A. The higher fraction of the HMRs after route A appears to be consistent with a continuous inclination of grains toward the extrusion

direction during multipass ECAE without rotations. During this process, the HAB area increases not only due to grain subdivision, but also due to significant geometric changes of the grain shape.[17,18] Colonies of pronounced shear bands, indicative of plastic instabilities, introduce additional HABs in sample A.

B. *Recrystallization of ECAE-Deformed Copper during Room-Temperature Storage*

Recrystallized grains, often containing twin boundaries, were observed in this work for samples processed by both ECAE routes. The presence of large recrystallized grains in as-deformed ECAE samples (*i.e.*, without subsequent annealing) has previously been reported for both high-purity[20] and commercially pure copper.[7–10] Some researchers attribute their appearance to dynamic recrystallization during ECAE.[8,21] To verify whether this could be the case for the samples investigated in the present work, original TEM micrographs recorded from the samples shortly after their processing were thoroughly re-inspected, specifically searching for signs of recrystallization. Out of many TEM images sampling several thousands of cells and subgrains, only one equiaxed 500-nm grain containing a morphologically distinguishable ''annealing'' twin was found. Several equiaxed crystallites of a similar size were free of dislocations but did not contain twins. Such subgrains could be potential nuclei for recrystallization during room-temperature storage. These observations can be compared to a number of large recrystallized grains easily detected in the TEM foils after storage that were also re-examined in the TEM for the present experiment (Section II). It is therefore considered that most of the recrystallized grains observed in this study developed not during, but after ECAE processing, and grew to a significant size during storage at room temperature. These grains were frequently found at local heterogeneities such as shear bands and intersections of extended boundaries.

The overall fraction of recrystallized material is low for both samples, though a higher fraction is found in the route Bc sample (Table I). This contrasts with the observation that the route A sample exhibits a smaller average spacing and a higher fraction of HABs. However, there is also a very large variation in the recrystallized volume fraction observed from region to region in sample B, as indicated by the data collected from the BSE and EBSD investigations shown in Figure 7. Additionally, the EBSD analysis shows that in both samples the deformed microstructure is heterogeneous, divided into HMRs and LMRs. The recrystallization nuclei seem to be predominantly located inside the HMRs, although again this observation by itself cannot explain the differences in the recrystallization behavior, as the route A sample shows a higher fraction of HMRs than the route Bc sample. Nucleation of recrystallization is known to be very much a localized phenomenon and it is reasonable to expect that the number of nuclei forming will be influenced by the local heterogeneity of the deformed microstructure. While a complete understanding of the recrystallization behavior of the given samples at present is not possible, the results obtained suggest that both the amount and type of heterogeneity must be considered when analyzing the onset of recrystallization in heavily deformed materials.

C. *Implication of Microstructural Heterogeneity for Characterization*

The results presented in this work demonstrate that the microstructure of copper after eight ECAE passes cannot be described as homogeneous. For sample A, local heterogeneities were observed in the deformed microstructure. However, over a large scale the microstructure and texture appeared fairly uniform. It is significant that an EBSD map from only one region represented well the characteristic shear texture measured in large sample areas after route A ECAE. Both local and macroscopic heterogeneities are revealed in the sample extruded using route Bc. Although the maps shown in Figures 1 and 2 cover areas of identical size, crystallographic orientations from the region mapped in sample B showed one dominant component, resembling the texture of a deformed single crystal. Areas with this dominant component are combined with regions characterized by large fractions of HABs. It should be noted that all the data reported in this article concern the microstructure along the center line of each ECAE billet, and that the observed heterogeneity is in addition to any variation in the microstructure over the sample length scale (*e.g.*, from the top to the bottom of the billet[22] or from the end to the middle[23]).

The variations between different regions in sample B are in fact so significant (Figure 5) that neither the texture, nor the microstructure analyzed in a small single region can be considered typical or representative. This observation alone could explain the controversy concerning the efficiency of microstructural refinement in terms of HAB formation for route A compared to route Bc. Information gained from small investigated areas, either based on the analysis of SAD patterns or from investigations of small selected regions in the TEM or using EBSD, is simply insufficient for characterizing the efficiency of grain subdivision in such heterogeneous samples. In some regions the microstructure may be described as uniform, containing almost equiaxed subgrains separated by HABs, but if larger areas are sampled it becomes evident that such structures do not represent the microstructure of the entire sample.

Interestingly, the HAB fraction obtained for the sample B in the present EBSD experiment was similar to that measured using TEM,[11,12] which is perhaps surprising considering the heterogeneity observed and the fact that misorientations <2 deg have been ignored in the EBSD analysis. Although the similar measured HAB fractions may have arisen both from the much lower TEM measurement statistics and from the limited angular resolution of the EBSD technique, it should be pointed out that in the previous TEM investigation special care was taken to characterize the microstructure in several regions chosen at random. The similarity of

the TEM and EBSD data indicate therefore that this characterization approach allows a TEM investigation to capture the heterogeneous nature of the microstructure. For example, similar large variations in the fraction and spacing of the HABs were seen in the TEM investigation.[11,12] Thus, the data gathered in the present FEGSEM/EBSD study nicely complement the existing TEM data. Therefore, regardless of the technique used for characterization of microstructures produced by ECAE, several regions should always be inspected to take account of the fact that the microstructure varies from region to region.[24] As each technique has its own limitations, more comprehensive information can be obtained by a combination of different techniques. By using proper TEM analysis the arrangement and characteristics of all boundaries, including those of low-misorientation angles, can be characterized very accurately, while the EBSD technique provides vital information to establish the length scales of the sample heterogeneities.

V. CONCLUSIONS

The microstructure along the center line of two copper samples obtained after eight ECAE passes using either route A or route Bc through a 90 deg die has been inspected in this work after long-term room-temperature storage. The following conclusions are reached.

1. Samples produced using both route A and Bc showed a significant amount of microstructural heterogeneity. In some areas (HMRs) there is a high density of HAB misorientations, whereas in other areas (LMRs) the microstructure contains only low misorientations and is more typical of a low strain-deformed microstructure. An analysis of the deformed microstructure in terms of LMRs and HMRs allows a quantitative description of this heterogeneity.
2. The microstructure in the route A sample is more refined than that in the route Bc sample, as indicated by a finer average HAB spacing, and a larger average HAB fraction. The greater refinement in the route A sample arises in part from the greater HMR area fraction in this sample. The latter appears to be consistent with the significant geometric changes of the grain shape occurring during route A ECAE, which additionally increases the HAB area.
3. Recrystallized grains are seen in both ECAE samples after storage at room temperature for 8 years. The recrystallized grains are observed mostly in the HMRs. The route Bc sample contains a higher fraction of recrystallized material and also exhibits a much greater local variation in the fraction of recrystallized material, showing that the amount of recrystallization is not simply related to the HMR area fraction.
4. The significant heterogeneities present in the ECAE-deformed samples imply that many regions have to be carefully inspected to take into account local variations in the microstructure. It is suggested that different characterization techniques should be combined to enable more comprehensive information about microstructural parameters after ECAE.

REFERENCES

1. V.M. Segal: *Mater. Sci. Eng. A*, 1995, vol. 197, pp. 157–64.
2. S. Ferrasse, K.T. Hartwig, R.E. Goforth, and V.M. Segal: *Metall. Mater. Trans. A*, 1997, vol. 28A, pp. 1047–57.
3. J. Schamp, B. Verlinden, and J. Van Humbeeck: *Scripta Mater.*, 1996, vol. 34, pp. 1667–72.
4. T. Ichikawa, S. Aoyama, T. Takahashi, and H. Nagayama: *Hitachi Cable Rev.*, 2000, vol. 19, pp. 47–50.
5. N.A. Akhmadeev, N.P. Kobelev, R.R. Mulyukov, Y.M. Soifer, and R.Z. Valiev: *Acta Metall. Mater.*, 1993, vol. 41, pp. 1041–46.
6. S. Komura, Z. Horita, M. Nemoto, and T.G. Langdon: *J. Mater. Res.*, 1999, vol. 14, pp. 4044–50.
7. Y. Estrin, N.V. Isaev, S.V. Lubenets, S.V. Malykhin, A.T. Pugachov, V.V. Pustovalov, E.N. Reshetnyak, V.S. Fomenko, L.S. Fomenko, S.E. Shumilin, M. Janecek, and R.J. Hellmig: *Acta Mater.*, 2006, vol. 54, pp. 5581–90.
8. A.L. Etter, T. Baudin, C. Rey, and R. Penelle: *Mater. Charact.*, 2006, vol. 56, pp. 19–25.
9. F.H. Dalla Torre, A.A. Gazder, C.F. Gu, C.H.J. Davies, and E.V. Pereloma: *Metall. Mater. Trans. A*, 2007, vol. 38A, pp. 1080–95.
10. F.H. Dalla Torre, A.A. Gazder, E.V. Pereloma, and C.H.J. Davies: *J. Mater. Sci.*, 2007, vol. 42, pp. 9097–111.
11. O.V. Mishin, D. Juul Jensen, and N. Hansen: *Proc. 21st Risø Int. Symp. on Materials Science: Recrystallization-Fundamental Aspects and Relations to Deformation Microstructure*, Risø National Laboratory, Roskilde, Denmark, 2000, pp. 445–49.
12. O.V. Mishin, D. Juul Jensen, and N. Hansen: *Mater. Sci. Eng. A*, 2003, vol. 342, pp. 320–28.
13. I.J. Beyerlein, R.A. Lebensohn, and C.N. Tomé: *Mater. Sci. Eng. A*, 2003, vol. 345, pp. 122–38.
14. O.V. Mishin and X. Huang: *Mater. Sci. Forum*, 1999, vols. 294–296, pp. 401–04.
15. R.Z. Valiev and T.G. Langdon: *Prog. Mater. Sci.*, 2006, vol. 51, pp. 881–981.
16. O.V. Mishin, X. Huang, J.R. Bowen, and D. Juul Jensen: *Proc. 22nd Int. Symp. on Materials Science: Science of Metastable and Nanocrystalline Alloys-Structure, Properties and Modelling*, Risø National Laboratory, Roskilde, Denmark, 2001, pp. 335–40.
17. A. Gholinia, P.B. Prangnell, and M.V. Markushev: *Acta Mater.*, 2000, vol. 48, pp. 1115–30.
18. M. Berta, P.J. Apps, and P.B. Prangnell: *Mater. Sci. Eng. A*, 2005, vols. 410–411, pp. 381–85.
19. Y.T. Zhu and T.C. Lowe: *Mater. Sci. Eng. A*, 2000, vol. 291, pp. 46–53.
20. G. Wang, S.D. Wu, L. Zuo, C. Esling, Z.G. Wang, and G.Y. Li: *Mater. Sci. Eng. A*, 2003, vol. 346, pp. 83–90.
21. W.H. Huang, C.Y. Yu, P.W. Kao, and C.P. Chang: *Mater. Sci. Eng. A*, 2004, vol. 366, pp. 221–28.

22. O.V. Mishin and J.R. Bowen: Risø National Laboratory for Sustainable Energy–DTU, Roskilde, Denmark, unpublished research, 2008.
23. J.R. Bowen, A. Gholinia, S.M. Roberts, and P.B. Prangnell: *Mater. Sci. Eng. A*, 2000, vol. 287, pp. 87–99.
24. O.V. Mishin, A. Godfrey, Q. Liu, and D. Juul Jensen: *Proc. 25th Int. Symp. on Materials Science: Evolution of Deformation Microstructures in 3D*, Risø National Laboratory, Roskilde, Denmark, 2004, pp. 445–51.